Journal Name

Adsorption and Growth of Palladium Clusters on Graphdiyne[†]

A. Seif,[a,b] M.J. López,[*a] A. Granja-DelRío[a], K. Azizi[b], and J.A. Alonso[a]

The density functional formalism has been used to investigate the stability and the properties of small palladium clusters supported on graphdiyne layers. The large triangular holes existing on the graphdiyne structure provide efficient sites to hold the clusters at small distances from the plane of the graphdiyne layer. The cluster adsorption energies, between 3 and 4 eV, are large enough to maintain the clusters tightly bound to the triangular holes. The competition between dispersion of Pd atoms on graphdiyne and growth of Pd clusters in the triangular holes of the layer is also discussed. In addition, the triangular holes can be simultaneously decorated with clusters on both sides. This indicates that palladium clusters could be used to build nanostructures formed by stacked graphdiyne layers with tailored interlayer distances controlled by the size of the clusters. The size of the clusters also controls the electronic HOMO-LUMO gap of the material.

1 Introduction

An important and common process in the industrial and pharmaceutical areas is catalysis. Often, clusters of transition metals (TM) supported on appropriate surfaces are the active catalysts, and the understanding of the cluster-support interaction is of great scientific and technological interest. Also, for many other purposes, the presence of adsorbed clusters can modify the electronic and magnetic properties of the substrate system[1]. There are some challenges regarding the adsorption of molecular species on supported metal clusters, related to the coupling of the clusters with the substrate[2–9]. For instance, an important issue is to reduce the TM contamination occurring during desorption of the molecular species; that is, preventing desorption of TM-molecule complexes. Evidently, a strong binding between the TM clusters and the supporting surface will result in a lower contamination of TM[6]. Also, a strong TM-surface binding will decrease the metal migration and aggregation on the substrate, which is a big challenge in fuel cells[10]. Therefore, designing stable TM-supported systems as efficient frames for adsorption of chemical species is relevant. Nowadays, because of their unique advantages of light weight, flexibility, diverse and economical methods of fabrication, novel carbon allotropes have been given a lot of attention as substrates. In addition, those carbon allotropes are generally stable under different working conditions and allow

for an ecological recovery of the catalytic metal by simply burning off the carbon. In this way, fullerenes[11], carbon nanotubes[12] and graphene[13] have been synthesized and applied in diverse fields. However, the applications of the first two have been limited mostly due to the unavailability of their inner surfaces, and particular attention has been dedicated to graphene. In fact, graphene is a good model for the inner surfaces of the pores in porous carbons[14].

Taking palladium as an example, it is known that Pd atoms and clusters bind much stronger to graphene vacancies than to pristine graphene[6]. As this effect could be assigned to a different local electronic structure induced by the absence of carbon atoms at the vacancies, we became motivated to look at one of the newest synthesized allotropic forms of carbon, graphdiyne (GDY)[15]. This is a layered framework formed by benzoic rings connected by very stable carbon chains containing diacetylenic linkages (see Figure 1). The structure presents an ordered regular arrangement of large triangular holes in the planar layers, with the sides of the triangle being linear $-C\equiv C-C\equiv C-$ chains with the two ends linked to the hexagonal benzoic rings. This arrangement leads to remarkable electronic and optical properties that are quite different from those of graphene, such as a natural band gap opening due to the asymmetric π conjugation[16], high third-order nonlinear optical susceptibility[17], and high fluorescence efficiency[18]. Consequently, promising applications of GDY are expected in electrode materials[19], semiconductor devices[20], hydrogen storage[21], gas separation[22], lithium storage[23], solar cells[24], etc.

Pan and coworkers[25] have reported density functional (DFT) calculations investigating the interfaces between graphdiyne and

[a] Departamento de Física Teórica, Atómica y Optica, Universidad de Valladolid, 47011 Valladolid, Spain.
[b] Department of Chemistry, Faculty of Science, University of Kurdistan, Sanandaj, Iran.
[*] Corresponding author. Tel:+34 983-184436. E-mail: maria.lopez@fta.uva.es

metallic palladium, proposing that this contact could be effective for graphdiyne-based devices, especially in field effect transistors. Using experimental methods, Qi et al. have concluded that GDY can be used as an effective reducing agent and stabilizer for electroless deposition of Pd nanoparticles[26], and it was also discovered that graphdiyne could be an excellent substrate to replace graphite or other pure carbon matrices for stabilizing Pt nanoparticles[27].

A study of the electronic and adsorption properties of Pd clusters supported on GDY, and a comparison with the corresponding results for adsorption of the same clusters on pure and defective graphene should be very valuable. Palladium shares many interesting properties with platinum, and it was recently found that hyper-cross-linked polystyrene (HPS) can be efficiently used to control the growth, size and shape of metal nanoparticles such as Pt and Pd[28]. However, palladium is lighter (and less expensive) than platinum. Then, considering that the adsorbate to adsorbent weight ratio plays an important role in the adsorption of molecular species, Pd should also be favorable in many cases. The present work presents a theoretical analysis of the structure and the electronic properties of palladium clusters deposited on GDY layers. The transition from planar to three-dimensional structures of the deposited Pd clusters is identified and compared to the corresponding case of deposition on graphene. The competition between the dispersion of Pd atoms deposited on GDY and the clustering of the of the Pd atoms and growth of Pd clusters in the triangular holes of the layer is also discussed. Finally, simultaneous deposition of clusters on both sides of the GDY layer is also explored. Because small metal particles have a higher fraction of surface atoms than larger particles, dispersed small particles can be advantageous in catalysis and in adsorption processes.

2 Computational method

Density functional calculations were carried out using the DACAPO code[29] and ultrasoft pseudopotentials. A basis set of plane waves is used to expand the Kohn-Sham wave functions and the electronic density, with cutoff values of 350 eV and 1000 eV, respectively. The substrate, GDY layer, was simulated as a periodically repeated unit cell consisting of 72 carbon atoms in the (x, y) plane (see Fig. 1). To minimize interactions between periodic images, the cell parameter c in the z direction was fixed at 14 Å. Integrations over reciprocal space are based on a Monkhorst-Pack grid with $2\times2\times1$ k-points, as a sufficiently large cell has been considered here. The value of c, the cutoffs, and the Monkhorst-Pack grid were taken to guarantee adsorption energies with a numerical precision of 0.005 eV. Optimization of geometries was lasted until the forces on the atoms were lower than 0.05 eV/Å. The ultrasoft pseudopotential for Pd uses a Kr-like core. The exchange-correlation energy is calculated with the Perdew-Wang PW91 functional[30], within the generalized gradient approximation (GGA). Since this functional does not incorporate dispersion interactions, we have also performed dispersion corrected density functional calculations using Grimme's DFT-D3 corrections[31] to the PBE[32] functional for exchange-correlation. Both, the calculated DFT-PW91 and DFT-PBE-D3 energies are provided to asses the effect of the dispersion interactions. Cluster adsorption ener-

gies were calculated in different ways:

$$E_{\text{add}}(\text{Pd}) = E(\text{GDY} - \text{Pd}_{n-1}) + E(\text{Pd}) - E(\text{GDY} - \text{Pd}_n) \quad (1)$$

$$E_{\text{ads}}(\text{Pd}_n) = E(\text{GDY}) + E(\text{Pd}_n) - E(\text{GDY} - \text{Pd}_n) \quad (2)$$

$$E_{\text{form}}(\text{Pd}_n) = [E(\text{GDY}) + n\,E(\text{Pd}) - E(\text{GDY} - \text{Pd}_n)]/n \quad (3)$$

where $E(\text{GDY-Pd}_n)$, $E(\text{GDY})$ and $E(\text{Pd}_n)$ represent the total energies of the combined system GDY-Pd$_n$, clean GDY and isolated Pd$_n$ clusters, respectively. In this way, $E_{\text{add}}(\text{Pd})$ is the energy released by adding a Pd atom to the supported Pd$_{n-1}$ cluster; that is, the adsorption energy of the additional Pd atom, and it helps to understand the growth of the supported cluster. E_{ads} is the adsorption energy of the Pd$_n$ cluster on GDY. Finally, $E_{\text{form}}(\text{Pd}_n)$ is the energy of formation, per Pd atom, of the supported GDY-Pd$_n$ system starting from clean GDY and n isolated Pd atoms. In these definitions, the system becomes more stable the larger is the value of the left hand side. The electronic energy gap variation, ΔE_{gap}, for any GDY-Pd$_n$ system is defined by $E_{\text{gap}}(\text{GDY-Pd}_n)$ $-E_{\text{gap}}(\text{GDY})$, where E_{gap} is the difference between the energies of the lowest unoccupied molecular orbital, LUMO, and the highest occupied molecular orbital, HOMO. ΔE_{gap} is an indicator of the change in the electronic structure due to the cluster adsorption.
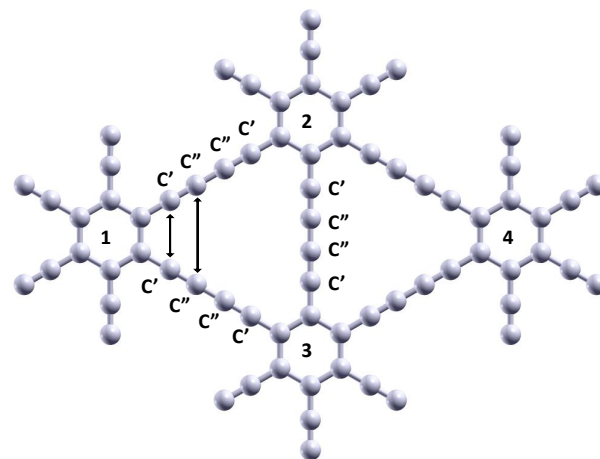
3 Results and discussion

Fig. 1 Optimized structure of the unit cell of GDY used in the calculations. The C'-C' and C"-C" distances near the benzenic rings, marked as double arrows, are 2.82 Å and 4.05 Å, respectively.

A supercell of single-layer graphdiyne, Fig. 1, was considered to simulate the substrate. The optimized lattice constant is 9.7 Å, in good agreement with other DFT calculations[33–35]. Due to the diversity in the hybridization of the carbon-carbon bonds in the $-\text{C}\equiv\text{C}-\text{C}\equiv\text{C}-$ chains in graphdiyne, the bond lengths along the chain are different: 1.39, 1.23, 1.33, 1.23, and 1.39 Å, aligned from one carbon hexagon to the nearest carbon of an adjacent hexagon. In contrast, the carbon-carbon bond lengths in the carbon hexagons are larger, with an average value of 1.43 Å. Compared with graphene, the diversity of hybridization and bond lengths in GDY results in different properties. For later conve-

Table 1 Addition, adsorption and formation energies (in eV), and some relevant (averaged) interatomic distances (in Å) of palladium clusters adsorbed on GDY. For each system the first row provides the energies calculated with the dispersion corrected formalism DFT-PBE-D3, and the second row in parenthesis gives the energies calculated with the DFT-PW91 formalism that does not incorporate dispersion interactions.

System	E_{add}	E_{ads}	E_{form}	$d(Pd-C')$ $(d(Pd-C''))$	$d(C'-C')$	$d(C''-C'')$
GDY				-	2.82	4.05
GDY-Pd	2.54 (2.49)	2.54 (2.49)	2.54 (2.49)	2.08(2.19)	2.68	4.23
GDY-Pd$_2$	2.45 (2.40)	3.74 (3.59)	2.49 (2.45)	2.10(2.25)	2.72	4.28
GDY-Pd$_3$	3.01 (2.96)	4.41 (4.14)	2.67 (2.62)	2.06(2.27)	2.72	4.41
GDY-Pd$_4$	2.09 (2.03)	3.56 (3.19)	2.52 (2.47)	2.10(2.36)	2.65	4.38
GDY-Pd$_5$	2.90 (2.82)	4.13 (3.65)	2.60 (2.54)	2.09(2.38)	2.66	4.48
GDY-Pd$_6$	2.57 (2.45)	3.97 (3.40)	2.59 (2.53)	2.11(2.49)	2.65	4.35
GDY-Pd$_{13}$	-	4.82 (3.83)	2.73 (2.64)	2.18(2.23)	2.84	4.27
Pd$_n$ and Pd adsorbed on different triangular holes of GDY						
GDY-Pd-Pd	2.50 (2.45)	-	2.52 (2.47)	2.09(2.19)	2.69	4.23
GDY-Pd$_3$-Pd	2.81 (2.69)	-	2.70 (2.63)	2.54(2.12)	2.98	3.84
Pd$_n$ adsorbed on both sides of GDY						
GDY-2Pd$_6$*	-	4.05 (3.29)	2.61 (2.51)	2.15(2.82)	2.55	4.91
GDY-2Pd$_6$**	-	4.13 (3.17)	-	2.15(2.82)	2.55	4.91
GDY-2Pd$_{13}$*	-	5.49 (4.05)	2.78 (2.66)	2.32(2.38)	2.91	4.27
GDY-2Pd$_{13}$**	-	6.16 (4.28)	-	2.32(2.38)	2.91	4.27

* E_{ads}^1 (Pd$_n$) of eq. (4)
** E_{ads}^2 (Pd$_n$) of eq. (5)

nience, the four carbon atoms along the $-C\equiv C-C\equiv C-$ chains are labelled C', C", C" and C', respectively, as indicated in Fig 1. The distance between the two C' atoms close to a hexagonal ring, indicated by a double arrow in Fig. 1, is $d(C'\text{-}C') = 2.82$ Å, and the distance between the two C" atoms, also indicated by a double arrow, is $d(C''\text{-}C'') = 4.05$ Å.

3.1 Pd cluster growth on GDY

The adsorption behavior of palladium clusters and their growth on GDY is now discussed starting with the adsorption of a single Pd atom. In order to find the most stable position for a Pd atom on GDY, many initial locations in the big triangular and small hexagonal holes were explored and relaxed, and the most stable configuration found corresponds to the Pd atom inside the triangular hole, in the position shown in Fig. 2, symmetrically bound to the nearest C' and C" atoms of two carbon chains of the triangle. The adsorption binding energy is $E_{ads} = 2.54$ eV. The addition and formation energies are, evidently, equal to the adsorption energy in this case. The Pd atom fits quite well in the GDY plane, being only 0.04 Å above the plane. The bond distances Pd-C' and Pd-C" are 2.08 Å and 2.19 Å, respectively, in good agreement with previous results by Lu et al.[36], who obtained values of 2.07 Å and 2.17 Å for those two distances. Adsorption, addition and formation energies of all the Pd clusters studied, as well as the relevant bond lengths and interatomic distances are shown in Table 1. The distortion of the structure of GDY induced by the adsorption of the Pd atom is non negligible. The C'-C' distance near the hexagonal ring 1 decreases by 0.14 Å ($d(C'\text{-}C') = 2.68$ Å), while the C"-C" distance increases by 0.18 Å ($d(C''\text{-}C'') = 4.23$ Å), and so the two $-C\equiv C-C\equiv C-$ chains near the adsorbed Pd atom become a bit distorted.

The magnetic moment of GDY-Pd is $M = 0$ (magnetic moments of the all systems studied are given in Table 2). Regarding the results obtained for adsorption of atomic Pd on pristine graphene[2], the Pd atom sits above a C-C bond, at a vertical distance of 2.22 Å, with adsorption energy of 1.09 eV. In the case of the graphene vacancy[6], the Pd atom sits at a distance of 1.56 Å above the vacancy center, with adsorption energy of 5.13 eV. In summary, the adsorption energy of Pd on GDY is intermediate between the other two cases, and the distance of Pd to the carbon plane is the lowest; that is, the Pd atom is nearly in-plane. The close approach of the Pd atom to the carbon plane results in a stronger interaction of Pd with GDY compared to pristine graphene; however, it is less intense compared to the interaction with the vacancy, because the vacancy has reactive dangling bonds.

Starting with the lowest energy configuration for adsorbed Pd, a second Pd atom was added in different positions on both sides of the GDY plane and all those initial configurations of the system were relaxed. The most stable position of the dimer is shown in Fig. 2, with the second Pd atom near a second corner of the triangular hole, and the addition energy is $E_{add} = 2.45$ eV. The two Pd atoms stand a bit out of the GDY plane, by 0.6 Å, but on opposite sides from that plane. The Pd-Pd distance is 2.75 Å. This bond length is elongated by 0.23 Å with respect to the free Pd_2 dimer ($d = 2.52$ Å), as a consequence of the interaction of the Pd

Table 2 Energy band gaps, E_{gap}, of GDY-Pd_n, change in the gap with respect to clean GDY, and magnetic moment M of GDY-Pd_n

System	E_{gap} (eV)	$\triangle E_{gap}$ (eV)	M (μ_B)
GDY	0.93	-	0
GDY-Pd	0.79	-0.14	0
GDY-Pd_2	0.35	-0.58	0
GDY-Pd_3	0.46	-0.47	0
GDY-Pd_4	0.26	-0.67	0
GDY-Pd_5	0.25	-0.68	0
GDY-Pd_6	0.07	-0.86	0
GDY-Pd_{13}	0.18	-0.75	0
Pd_n and Pd adsorbed on different triangular holes			
GDY-Pd-Pd	0.70	-0.23	0
GDY-Pd_3-Pd	0.51	-0.42	0
Pd_n adsorbed on both sides of GDY			
GDY-$2Pd_6$	0.07	-0.86	2
GDY-$2Pd_{13}$	0.03	-0.90	2

atoms with GDY. The magnetic moment of the system is $M = 0$. The C'-C' and C"-C" distances increase with respect to the case of a single adsorbed Pd atom. The average of the two relevant C'-C' distances near the Pd atoms is 2.72 Å, and the average of the two C"-C" distances is 4.28 Å. The first one is still smaller than the value $d(C'\text{-}C') = 2.82$ Å in clean GDY. In pristine graphene, Pd_2 forms on the same side of the carbon plane[2]; in contrast, on defective graphene[37] and on GDY, Pd_2 samples both sides of the flake, what is quite interesting for the adsorption of gases. We also found a second low-lying energy minimum of GDY-Pd_2 with the two Pd atoms on the same side of the GDY plane, and energy 0.5 eV above the ground state.

Adding a third Pd atom leads to the very symmetrical configuration in Fig. 2. The Pd atom occupies the third corner of the big triangular hole, as it could be expected. Interestingly, the three Pd atoms are close to the GDY plane, the average height is 0.23 Å, and it can be appreciated in the Figure that the distortion of the surrounding carbon chains is larger than in the two previous cases. Averages of C'-C' and C"-C" distances in Table 1 show an additional increase of d(C"-C"). The large addition energy, E_{add} = 3.01 eV, reveals the contribution of the Pd-Pd bonds. This bonding contribution occurs because the Pd-Pd distances, 2.57, 2.60 and 2.61 Å, are close to the Pd-Pd distance in the isolated Pd_3 cluster[2], $d(Pd\text{-}Pd) = 2.56$ Å, and this effect compensates for the distortion energy of the carbon chains. The parallel orientation of Pd_3 with respect to the GDY plane is at variance with the adsorption on pristine graphene or on a graphene vacancy: in those cases the triangular Pd cluster is perpendicular to the plane of carbon atoms[5,6]. We notice that the energy of the next low-lying minimum, corresponding to a triangular configuration of Pd_3 with vertical orientation similar to those occurring on pristine and defective graphene, is 0.5 eV above the ground state.

Similar to the isolated Pd_4 cluster[38] and Pd_4 cluster supported on pristine[2] and defective graphene[6], Pd_4 with tetrahedral struc-
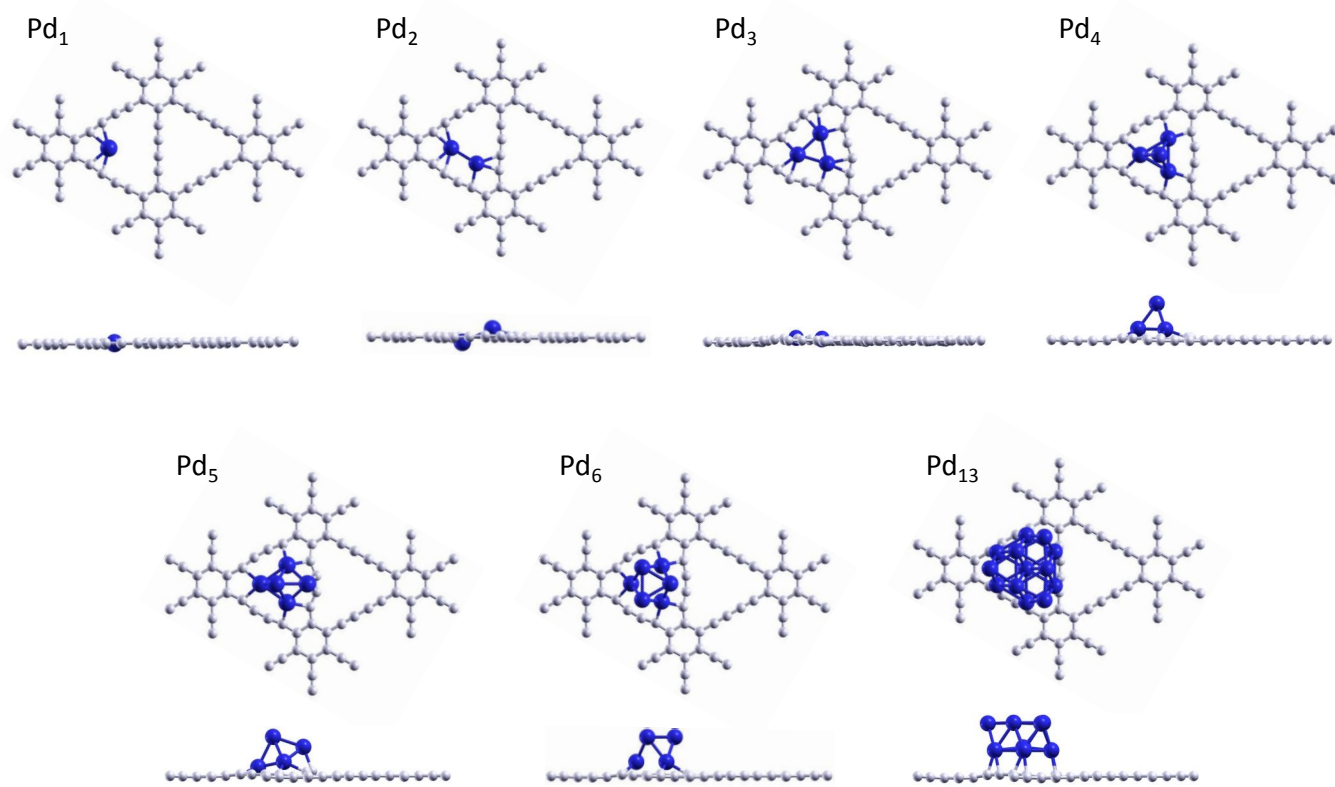
Fig. 2 Top and side views of the ground state geometries of GDY-Pd$_n$ with $n = 1-6$, 13.

ture is the first three-dimensional structure for Pd$_n$ clusters on GDY. One face of the tetrahedron sits on the GDY plane (see Fig. 2) . The position of the three Pd atoms of that face relative to the triangular hole is similar to that seen above for Pd$_3$, but the atoms are at an average height of 0.95 Å above the GDY plane. The addition energy of the fourth Pd atom, E_{add} = 2.09 eV, is due mostly to Pd-Pd bonding, because the fourth Pd atom is well above the GDY plane. Actually, the interaction of the fourth Pd atom with the other three allows the Pd$_3$ triangle to move up to form the tetrahedron. At the same time the interatomic Pd-Pd distances experience an expansion towards values 2.67 - 2.69 Å, close to those in free Pd$_4$ [2].

The lowering of the addition energy between Pd$_3$ and Pd$_4$ is an interesting feature. Although adding the fourth atom provides substantial Pd-Pd bonding, separating Pd$_3$ from its favorable position close to the pore plane reduces the interaction between the cluster and GDY. The closest palladium-carbon distances (average d(Pd-C') = 2.10 Å), are smaller than those for Pd$_4$ on pristine graphene (2.3-2.4 Å), so the interaction is still higher.

The ground state structure of Pd$_5$ on GDY is obtained by capping the triangular face on the right hand side of the tetrahedron, as shown in Fig. 2. Then, the two Pd atoms near the hexagonal rings 2 and 3 move a bit towards the hexagonal ring 1. In this way, the distorted trigonal bipyramid shown in Fig. 2 is obtained for supported Pd$_5$ (in fact, the structure is midway between a trigonal bipyramid and a square pyramid). The addition energy is E_{add} = 2.90 eV. The position of the cluster is peculiar: three Pd atoms, forming a face of that distorted trigonal bipyramid, sit

on top of the triangular hole in a configuration similar to those found in Pd$_3$ and Pd$_4$, that is, near the three vertices of the pore. However, this triangular face is not parallel to the GDY plane; the heights of the three Pd atoms above the GDY plane are 0.76, 1.20 and 1.20 Å, and this indicates that the face is tilted with respect to the GDY plane. The shape of the distorted structure of supported Pd$_5$ is in between the two lowest energy structures of isolated Pd$_5$, the trigonal bipyramid and the square pyramid [2]. In fact, the second most stable isomer of Pd$_5$ on GDY is the square pyramid, with energy 0.16 eV above the ground state. In comparison, the structure of Pd$_5$ on a graphene vacancy is also a trigonal bipyramid with the face in contact with the vacancy again tilted [6], as in the case of GDY. The structure of Pd$_5$ supported on pristine graphene is the square pyramid [5].

There are two main competing isomers for free Pd$_6$: the octahedral structure, OCT, which is the ground state, and the incomplete pentagonal bipyramid IPB (with an atom missing from the equatorial common base), with an energy 0.29 eV above the ground state [5]. The preferred structure of Pd$_6$ on GDY, as well as on other carbon materials (clean and defective graphene [6], and HPS) is the OCT structure. This structure is obtained with an addition energy E_{add} = 2.57 eV. As depicted in Fig. 2, Pd$_6$ on GDY rests on a triangular face. The position of this face on the triangular GDY hole is similar to the position of Pd$_3$, although the atoms are at a distance 1.22 Å above the GDY layer; the Pd-C' distances are 2.1 Å. The OCT structure, which is a singlet state, shows some distortion: the Pd-Pd distances in the triangular face facing GDY (the bottom face) are 2.95, 2.95 and 2.96 Å (average 2.95 Å), and the

Pd-Pd distances in the upper parallel face are 2.69, 2.69, 2.70 Å (average 2.69 Å). The Pd-Pd distances in the bottom face are enlarged by 10 per cent with respect to Pd-Pd distances in free Pd_6 (average 2.68 Å), and this enhancement is due to the interaction between Pd atoms with benzylic carbons C'. The energy of the second minimum, which is a spin triplet state, is 0.30 eV above the ground state.

The addition energies are collected together in Table 1. The Table also shows the formation energies and the cluster adsorption energies, defined in equations (3) and (2), respectively. There is a good correspondence in the trends of E_{add} and E_{form} as the size of the palladium cluster increases. The most salient feature shown by E_{ads} is that the largest adsorption energy occurs for Pd_3, which is the case when the triangular Pd_3 cluster is optimally close to the triangular hole. Actually, the most stable structures of Pd_3 to Pd_6 show a common feature, namely, their contact with GDY is through a triangular face, parallel to the GDY plane except for Pd_5, in which case the face is tilted. The situation for Pd_n supported on pristine graphene or on a graphene vacancy is different. In those cases Pd_3 is perpendicular to the substrate, and a variety of configurations occur for Pd_4-Pd_6.

The observed trend on GDY invites investigating larger clusters, and for this purpose we have focused on Pd_{13}. The structure of the isolated cluster is a bilayer formed by two fcc (111) planes with seven and six atoms, respectively[39,40]. The calculated lowest energy structure of Pd_{13} on GDY is shown in Fig. 2. The two Pd layers are parallel to the GDY plane, and the layer in contact with the substrate is the face having seven atoms: six Pd atoms sit on top of the carbon chains forming the boundary of the triangular hole, and the seventh Pd atom is in the center of the hole. The height of this layer above the GDY plane is 2.18 Å, the largest height of all clusters studied. On the other hand, the upper Pd layer forms a triangle with three atoms in positions whose projections on the GDY plane are near the vertices of the triangular hole and the projections of the other three atoms fall in the middle of the edges of that triangle. The distance between the two (111) planes of the cluster is 2.27 Å. This value is close to the interplanar spacing in Pd nanoparticles of size 4nm deposited on GDY and measured by high resolution transmission electron microscopy[26], d= 2.22 Å, and to the interplanar spacing in bulk fcc palladium, d=2.24 Å. This means that the effect of the GDY substrate on the interlayer spacing of the fcc-like Pd particles is small.

The spin magnetic moment of the free Pd_{13} cluster, 6 μ_B, quenches down to zero upon deposition of the cluster on GDY. In contrast, deposition of Pd_{13} on pristine graphene quenches only partially the moment and the magnetic moment of the supported cluster[41] is 4 μ_B. The adsorption energy of the cluster is E_{ads} = 4.82 eV. The adsorption energy of the clusters does not scale with the number of Pd atoms in contact with the substrate. For the three clusters having a triangular face in contact with GDY, Pd_3-Pd_6, the cluster adsorption energies vary between 3.56 and 4.41 eV. The adsorption energy of Pd_3, 4.41 eV, is larger than the adsorption energies of Pd_4, Pd_5 and Pd_6. The same lack of a systematic trend occurs for Pd_n clusters on pristine graphene[2–5]. We also conclude that the adsorption energies of Pd_n on GDY are intermediate between the adsorption energies on pristine and de-

fective graphene. As the number of vacancies in graphene is limited and these disappear at high temperature, GDY could be a more effective substrate to anchor clusters than graphene.

Inclusion of the van der Waals interactions leads to larger addition, adsorption and formation energies. Although van der Waals interactions are small, their net contribution increases as the size of the Pd cluster grows up. This can be appreciated in the addition energies $E_{add}(Pd)$ of Table 1. The dispersion contribution is 0.05 eV for the addition of the first Pd atom to GDY, and then grows up slowly, reaching a value of 0.12 eV for the addition of the sixth Pd atom. As a fraction of E_{add}, the dispersion contribution increases from 2 percent to 12 percent. This increase is due to the fact that the dispersion interactions are evaluated in the DFT-D3 method as a sum of pairwise terms, and a larger Pd cluster implies more terms. The adsorption energies E_{ads} reflect the same behavior. The van der Waals contribution to the adsorption energy of the Pd_n cluster increases from 0.05 eV for adsorption of a single Pd atom to 0.99 eV for the adsorption of Pd_{13}, or from 2 percent to 20 percent.

3.2 Competition between dispersion of Pd atoms and cluster growth on GDY

Palladium atoms deposited on a GDY layer can adsorb on the layer by binding to previously adsorbed Pd atoms, as shown in the previous section, and thus leading to the growth of Pd clusters. On the other hand, the successively deposited Pd atoms could also be adsorbed on different triangular holes, leading to the dispersion of the Pd atoms on the GDY layer. To shed light on the competition between these two processes, clustering and dispersion of Pd on GDY, we have investigated the adsorption of Pd on adjacent triangular holes. First we notice from the upper section of Table 1 that the addition energy of a second Pd atom next to a Pd atom preadsorbed on GDY (E_{add} = 2.45 eV) is almost equal to the adsorption energy of one palladium atom on the GDY layer (E_{ads} = 2.54 eV). These very similar energies suggest that it would be nearly equally favorable adding the second Pd atom on the same triangular hole or on a different triangular hole, thus the coverage of the GDY would tend to be uniform. The calculated addition energy of a second Pd atom on a different triangular hole than the first Pd atom, which amounts to 2.50 eV (see the middle section of Table 1), confirms that expectation. The most favorable position of the two Pd atoms in two adjacent pores is on opposite vertices of the respective triangular pores (see Fig. 3).
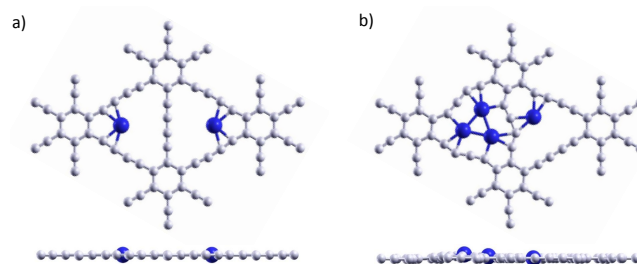

Fig. 3 Top and side views of the ground state geometries of a) two Pd atoms, and b) Pd_3 and one Pd atom, adsorbed on two adjacent triangular holes of GDY, respectively.

It is also of interest to study the competition between clustering and dispersion for preadsorbed Pd clusters, specially for the case when the transition between 2-dimensional, Pd_3, and 3-dimensional, Pd_4, clusters takes place. The triangular holes of GDY can hold a maximum of three Pd atoms in plane and thus the fourth Pd atom attached to the same pore forms a three dimensional Pd_4 cluster. Notice that the fourth Pd atom is not directly bound to the GDY layer. The addition energy of the fourth Pd atom to a preadsorbed Pd_3, 2.09 eV, is somewhat lower than the addition energy of that atom to a different triangular hole, 2.81 eV (see Fig. 3). This result can be understood because, as we showed in the previous subsection, the formation of the three dimensional Pd_4 cluster is accompanied by a lowering in the adsorption energy of the cluster (from 4.41 eV in Pd_3 to 3.56 in Pd_4) due to an increase in the overall distance between the cluster and the GDY layer. Therefore it is slightly more favorable to bind a Pd atom directly to the GDY layer in a different triangular hole than to grow a three dimensional Pd cluster. Overall, the two processes, dispersion of Pd atoms and growth of Pd clusters, can take place in the GDY layer. However, if preformed Pd clusters are deposited on GDY, they will adsorb with substantial adsorption energies as shown in the previous subsection. These conclusions are consistent with the experimental observation that the Pd nanoparticles of size 1.3 nm are fairly well dispersed on GDY[26].

3.3 Adsorption of Pd clusters on both sides of GDY

In order to investigate the efficiency of the GDY layer to anchor clusters on both sides of the big triangular hole simultaneously, two Pd_6 (or two Pd_{13}) clusters have been added. The lowest energy structures obtained are displayed in Fig. 4. The positions of the two Pd_6 (or two Pd_{13}) clusters are symmetrical with respect to the GDY plane. The projections of those positions onto the GDY plane are nearly the same as for single Pd_6 or Pd_{13} clusters. The cluster-GDY distance has increased to 1.34 Å for two Pd_6 (it was 1.22 Å for one Pd_6). However, the two Pd_{13} clusters are at the same distance (one on each side of the layer) from GDY, 2.21 Å, as the single Pd_{13}. We have calculated the cluster adsorption energies in two ways. In the first definition

$$E_{ads}^1(Pd_n) = [E(GDY) + 2E(Pd_n) - E(GDY - 2Pd_n)]/2 \quad (4)$$

is an average adsorption energy corresponding to the process of adding the Pd_n clusters on both sides of the GDY plane simultaneously. A second criterion can be used,

$$E_{ads}^2(Pd_n) = E(GDY - Pd_n) + E(Pd_n) - E(GDY - 2Pd_n)]/2 \quad (5)$$

corresponding to the process of adding the second cluster when the first one is already adsorbed. As shown in Table 1, the two adsorption energies are not equal: For Pd_6, E_{ads}^2 is a bit higher than E_{ads}^1, so the adsorption of the second cluster releases a larger amount of energy than the adsorption of the first one. The same effect can be noticed in that E_{ads}^1=4.05 eV and E_{ads}^2= 4.13 eV for Pd_6 are larger than the adsorption energy of the first Pd_6 cluster, 3.97 eV. This increase of the adsorption energy for the second Pd_6 cluster would not be expected on the basis of the increase of the
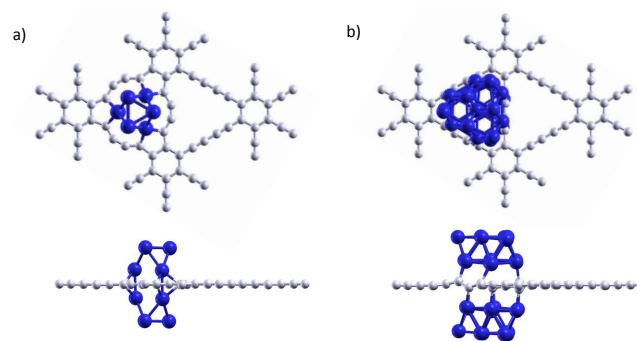

Fig. 4 Top and side views of the optimized structures of: (a) two Pd_6, and (b) two Pd_{13} clusters adsorbed on GDY.

GDY-Pd_6 distance, from 1.22 Å to 1.34 Å, upon adsorption of the second cluster. A larger distance usually leads to smaller interaction energies. However, the larger GDY-Pd_6 distance results in interatomic distances between neighboring Pd atoms across the pore of 2.68 Å, close to the interatomic distance of 2.75 Å in bulk Pd; in this way Pd-Pd bonding across the triangular hole is responsible for the increase of binding of the second Pd_6 cluster.

Similarly, in the case of Pd_{13}, E_{ads}^2 is a bit higher than E_{ads}^1. In this case, the distances between GDY and the two Pd_{13} clusters, 2.21 Å, are the same as for the adsorption of a single Pd_{13} cluster. The higher adsorption energy of the second Pd_{13} cluster, E_{ads}^2=6.16 eV, as compared with the adsorption energy of a single cluster, 4.82 eV, mainly reflects the effect of the Pd-Pd bonding across the triangular hole. Although the Pd-Pd distances across the triangular hole are larger than the bond distance in bulk Pd, the effect of the attractive tail of the effective interatomic potential is active. A part of this bonding effect is contributed by the dispersion interactions. The important conclusion from the whole discussion is that clusters can be attached on both sides of the GDY layer simultaneously with adsorption energies of about 4-6 eV. This result suggests that clusters can be employed to build nanostructures formed by GDY bilayers or multilayers with interlayer distances controlled by the intercalated clusters. A comparison of the C'-C' and C"-C" distances in GDY-$2P_6$ and GDY-$2Pd_{13}$ with those in GDY-Pd_6 and GDY-Pd_{13} reveals that the deformation of the carbon framework of the triangular holes is larger in GDY-$2P_6$ and GDY-$2Pd_{13}$. This can also be observed in the Pd-C' and Pd-C" distances in Table 1.

3.4 Electronic properties

Some electronic properties of all GDY-Pd_n and GDY-$2Pd_n$ systems are reported in Table 2, and the densities of states (DOS) of GDY, GDY-Pd and GDY-Pd_3 are shown in Fig. 5. The electronic band gap of pristine GDY is 0.93 eV. This value is intermediate between band gaps calculated using DFT with other exchange-correlation functionals (gaps in the range 0.4-0.5 eV)[33,42,43] and the value of 1.18 eV calculated by the hybrid B3LYP method[43]. A recent calculation within the many-body GW method predicts a gap of 1.10 eV[18]. The value of the gap is lowered to 0.79 eV in GDY-Pd, and Fig. 5 shows the presence of more electronic states in the region between -4 and 0 eV. The density of states projected

on the *d* levels of Pd (see Fig.5) shows that the additional levels in the region between -4 and 0 eV are mainly contributed by the *d* states of Pd. This trend continues for larger clusters and the development of a *d* band associated to the growth of the Pd clusters is clearly apparent from the projected density of states on the *d* levels of Pd in Fig.5. Moreover, the progressive lowering of the
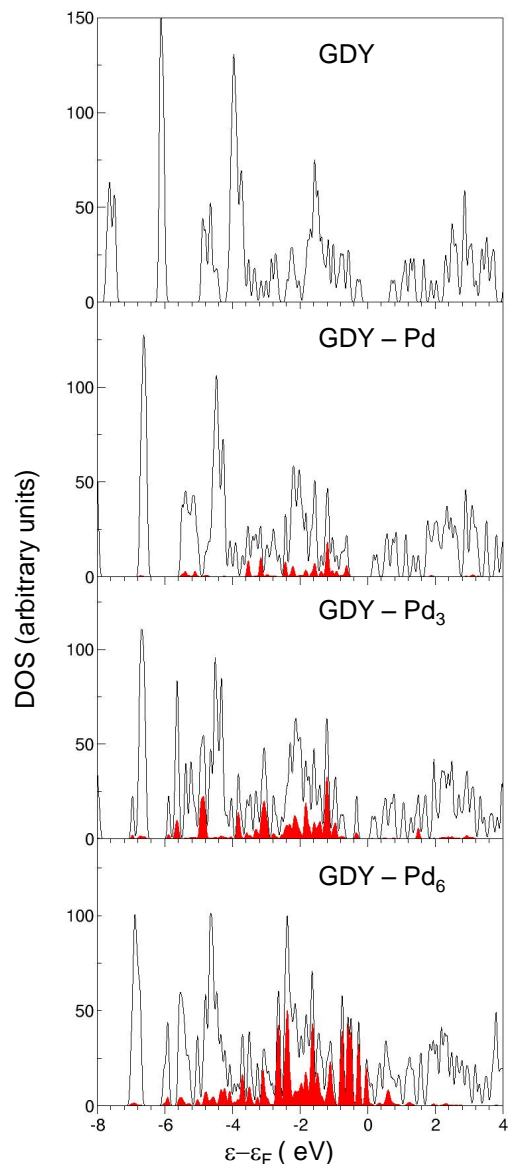

Fig. 5 Density of electronic states (black line) of GDY, GDY-Pd, GDY-Pd₃ and GDY-Pd₆. The projected density of states on the *d* levels of Pd is represented by the shadowed area in red. The energy region around the Fermi level, from -8 eV to 4 eV is shown in the figure. Notice that further bands corresponding to GDY without hybridization with Pd levels extend down to -19 eV (not shown). ε_F represents the Fermi energy.

width of the gap also continues as the anchored Pd_n cluster grows in size. This trend is attributed to the increasingly dominant effect of the Pd *d* states around the Fermi energy. Thus, the size of the Pd clusters can be used to modify the width of the band gap in a controlled way, a feature that could be useful for applications in sensing devices. On the other hand, the dispersion of

Pd atoms on different triangular holes of the GDY layer has only a minor effect in the electronic gap (the gap of GDY-Pd-Pd is 0.70 eV) with respect to the system with one adsorbed Pd atom, 0.79 eV. A similar behaviour is observed in the case of adsorption of a Pd atom in a triangular hole adjacent to another hole decorated with Pd_3. The gap in this case, 0.51 eV, is similar to that of the GDY-Pd₃ system, 0.46 eV.
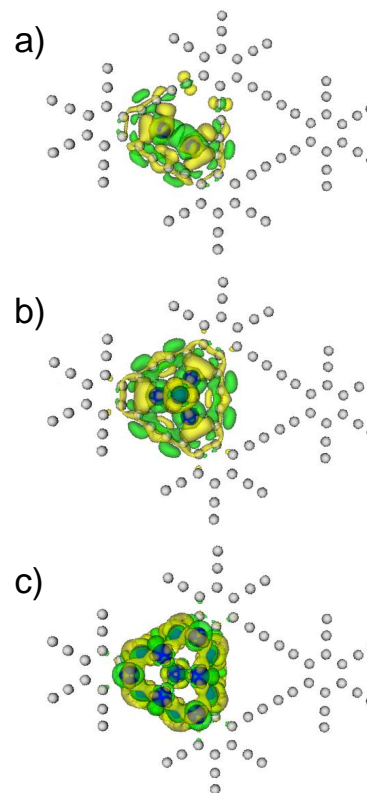

Fig. 6 Electron density redistribution in a) GDY-Pd₂, b) GDY-Pd₄ and c) GDY-Pd₁₃ resulting from cluster adsorption. Yellow and green colors indicate regions of enhancement and lowering of electron density, respectively.

The electron density redistribution, $\Delta\rho$, for adsorption of a Pd_n cluster on GDY, defined as

$$\Delta\rho = \rho(Pd_n \text{on} GDY) - \rho(Pd_n) - \rho(GDY) \qquad (6)$$

is given in Fig. 6 for GDY-Pd₂, GDY-Pd₄ and GDY-Pd₁₃. Yellow and green colors indicate regions of enhancement and lowering of electron density, respectively. The electron redistribution is quite complex, but an accumulation of electron density in the regions between the Pd atoms and the closest carbon atoms can be appreciated. Some polarization of the charge also occurs around the Pd atoms.

4 Summary and conclusions

Graphdiyne can serve as an efficient substrate to hold palladium atoms and clusters. The preferred positions for the Pd atoms and clusters are on the big triangular holes, at small distances from the graphdiyne layer plane. Those distances are not longer than 1.2 Å when the cluster size fits well in the triangular hole (up

to Pd_6 for the cluster sizes analyzed), and are longer than this value for larger cluster sizes (Pd_{13} in our case). Palladium atoms deposited on GDY can be dispersed in different triangular holes of the layer or may join together forming clusters. These two processes are nearly equally favorable. The cluster adsorption energies are between 3 and 4 eV, large enough to maintain the clusters tightly bound to the triangular holes, more so than the same clusters on pristine graphene. It is also feasible to dope graphdiyne simultaneously with clusters on the upper and lower sides of the same triangular hole, and the adsorption binding energies only decrease by a little (less than 10 percent). These properties indicate that Pd clusters (many other elements are expected to behave in the same way) can be used to build nanostructures in which graphdiyne layers are stacked with interlayer distances controlled at will by the size of the clusters. The size of the clusters also controls the electronic band gap of the material.

Conflicts of interest

There are no conflicts of interest to declare.

Acknowledgements

References

1 M. Mahmoodinia, P.-O. A. Strand and D. Chen, *J. Phys. Chem. C*, 2015, **119**, 24425.

2 I. Cabria, M. J. López and J. A. Alonso, *Phys. Rev. B*, 2010, **81**, 035403:1–5.

3 Q. Sun, Q. Wang, P. Jena and Y. Kawazoe, *J. Am. Chem. Soc.*, 2005, **127**, 14582–14583.

4 P. O. Krasnov, F. Ding, A. K. Singh and B. I. Yakobson, *J. Phys. Chem. C*, 2007, **111**, 17977–17980.

5 I. Cabria, M. J. López, S. Fraile and J. A. Alonso, *J. Phys. Chem. C*, 2012, **116**, 21179–21189.

6 M. J. López, I. Cabria and J. A. Alonso, *J. Phys. Chem. C*, 2014, **118**, 5081–5090.

7 I. López-Corral, S. Piriz, R. Faccio, A. Juan and M. Avena, *Applied Surface Science*, 2016, **382**, 80–87.

8 I. López-Corral, J. D. Celis, A. Juan and B. Irigoyen, *Int. J. Hydrogen Energy*, 2012, **37**, 10156–10164.

9 G. M. Yang, X. F. Fan, S. Shi, H. H. Huang and W. T. Zheng, *Appl. Surf. Sci.*, 2017, **392**, 936–941.

10 Y. Shao-Horn, W. C. Sheng, S. Chen, P. J. Ferreira, E. F. Holby and D. Morgan, *Topics in Catalysis*, 2007, **46**, 285.

11 H. W. Kroto, J. R. Heath, S. C. O'Brien, R. F. Curl and R. E. Smalley, *Nature*, 1985, **318**, 162–163.

12 S. Iijima, *Nature (London)*, 1991, **354**, 56–58.

13 K. S. Novoselov, A. K. Geim, S. V. Morozov, Y. Z. D. Jiang, S. V. Dubonos, I. V. Grigorieva and A. A. Firsov, *Science*, 2004, **306**, 666.

14 M. J. López, I. Cabria and J. A. Alonso, *J. Chem. Phys.*, 2011, **135**, 104706.1–9.

15 G. Li, Y. Li, H. Liu, Y. Guo, Y. Lia and D. Zhu, *Chemical Communications*, 2010, **46**, 3256–3258.

16 H. Bu, M. Zhao, H. Zhang, X. Wang, Y. Xi and Z. Wang, *J. Phys. Chem. A*, 2012, **116**, 3934–3939.

17 A. Bhaskar, R. Guda, M. M. Haley and T. G. III, *J. Am. Chem. Soc.*, 2006, **128**, 13972–13973.

18 G. Luo, X. Qian, H. Liu, R. Qin, J. Zhou, L. Li, Z. Gao, E. Wang, W.-N. Mei, J. Lu, Y. Li, and S. Nagase, *Phys. Rev. B*, 2011, **84**, 075439.

19 C. Sun and D. J. Searles, *J. Phys. Chem. C*, 2012, **116**, 26222–26226.

20 X. Qian, H. Liu, C. Huang, S. Chen, L. Zhang, Y. Li, J. Wang and Y. Li, *Sci. Rep.*, 2015, **5**, 7756.

21 H. J. Hwang, Y. Kwon and H. Lee, *J. Phys. Chem. C*, 2012, **116**, 20220–20224.

22 S. W. Cranford and M. J. Buehler, *Nanoscale*, 2012, **4**, 4587–4593.

23 C. Huang, S. Zhang, H. Liu, Y. Li, G. Cui and Y. Li, *Nano Energy*, 2015, **11**, 481–489.

24 J. Xiao, J. Shi, H. Liu, Y. Xu, S. Lv, Y. Luo, D. Li, Q. Meng and Y. Li, *Advanced Energy Materials*, 2015, **5**, 1401943.

25 Y. Pan, Y. Wang, L. Wang, H. Zhong, R. Quhe, Z. Ni, M. Ye, W.-N. Mei, J. Shi, W. Guo, J. Yang and J. Lu, *Nanoscale*, 2015, **7**, 2116–2127.

26 H. Qi, P. Yu, Y. Wang, G. Han, H. Liu, Y. Yi, Y. Li and L. Mao, *J. Am. Chem. Soc.*, 2015, **137**, 5260–5263.

27 Z.-Z. Lin, *Carbon*, 2015, **86**, 301–309.

28 A. Prestianni, F. Ferrante, E. M. Sulman and D. Duca, *J. Phys. Chem. C*, 2014, **118**, 21006.

29 dacapo, *See https://wiki.fysik.dtu.dk/dacapo for a description of the total energy code, based on the density functional theory (2009). Last accessed on January 2017.*

30 J. P. Perdew and Y. Wang, *Phys. Rev. B*, 1992, **45**, 13244–13249.

31 S. Grimme, J. Antony, S. Ehrlich and H. Krieg, *J. Chem. Phys.*, 2010, **132**, 154104:1–19.

32 J. P. Perdew, K. Burke and M. Ernzerhof, *Phys. Rev. Lett.*, 1986, **77**, 3865–3868.

33 M. Long, L. Tang, D. Wang, Y. Li, and Z. Shuai, *ACS Nano*, 2011, **5**, 2593–2600.

34 H. Zhang, M. Zhao, X. He, Z. Wang, X. Zhang and X. Liu, *Phys. Rev. C*, 2011, **115**, 8845–8850.

35 H. Zhang, X. He, M. Zhao, M. Zhang, L. Zhao, X. Feng and Y. Luo, *J. Phys. Chem. C*, 2012, **116**, 16634–16638.

36 Z. Lu, S. Li, P. Lv, C. He, D. Ma and Z. Yang, *Applied Surface Science*, 2016, **360**, 1–7.

37 A. Granja-DelRío, J. A. Alonso and M. J. López, *Computational and Theoretical Chemistry*, 2017, **1107**, 23–29.

38 M. Moseler, H. Häkkinen, R. N. Barnett and U. Landman, *Phys. Rev. Lett.*, 2001, **86**, 2545–2548.

39 L.-L. Wang and D. D. Johnson, *Phys. Rev. B*, 2007, **75**, 235405.

40 A. M. Köster, P. Calaminici, E. Orgaz, D. R. Roy, J. U. Reveles and S. N. Khanna, *Jour. Am. Chem Soc*, 2011, **133**, 12192–12196.

41 M. Blanco-Rey, J. I. Juaristi, M. Alducin, M. J. López and J. A. Alonso, *J. Phys. Chem. C*, 2016, **120**, 17357–17364.

42 N. Narita, S. Nagai, S. Suzuki and K. Nakao, *Phys. Rev. B*, 2000, **62**, 11146–11151.

43 K. Srinivasu and S. K. Ghosh, *Journ. Phys. Chem. C*, 2012, **116**, 5951–5956.